Electronic structure of Mn-doped III-V semiconductor quantum dots

Sucismita Chutia and A. K. Bhattacharjee
Laboratoire de Physique des Solides, UMR du CNRS, Université Paris-Sud, 91405 0rsay, France
(Received 18 July 2008; revised manuscript received 7 October 2008; published 13 November 2008)

The electronic structure of GaAs and InAs quantum dots (QDs) containing a single substitutional Mn impurity is investigated in the envelope-function formalism. The Mn impurity in these compounds is known to be a shallow acceptor in the configuration d^5+h and characterized by a strong antiferromagnetic *sp-d* exchange interaction between the hole (h) and the Mn ion. Our model for the hole states is based on the Luttinger Hamiltonian and the Coulomb potential with a central-cell correction that accounts for the observed binding energy and the effective g factor in the bulk. The binding energy as well as the exchange contribution is found to increase with decreasing QD size. However, in contrast with the case of spherical nanocrystals (NCs), the binding energy in lens-shaped self-assembled QDs in the low-confinement limit is lower than that in the bulk because of their highly anisotropic shape. With an on-center impurity, NCs retain the bulk T_d symmetry and the ground state is a $j=3/2$-like $\Gamma_8(T_d)$ level. In self-assembled QDs it splits into two doublets: Γ_6 ($|j_z|=1/2$) and Γ_7 ($|j_z|=3/2$) of D_{2d}, which mix in the presence of in-plane asymmetry, both belonging to Γ_5 of the reduced symmetry C_{2v}. The order and the splitting between the doublets depend on the degree of confinement and the strain-induced separation between the light- and heavy-hole valence bands. In lattice-matched GaAs/(Ga,Al)As QDs the ground-state doublet is $|j_z|=3/2$-like in the low-confinement limit. As the lateral size decreases there is a rapid crossover to a $|j_z|=1/2$-like ground state in QDs of typical sizes. On the other hand, in strained InAs/GaAs QDs the ground state is always $|j_z|=3/2$-like and the splitting relatively large. The *sp-d* coupling with the Mn spin $S=5/2$ finally leads to a splitting of the ground-state doublet into six doubly-degenerate levels. The components are close to one another as the effective exchange parameters are an order of magnitude smaller than in the bulk. Our results thoroughly contradict the previously adopted picture based on treating the confinement potential as a small perturbation to the bulk impurity levels. We also consider the lowest two-hole states: the ground state in InAs/GaAs QDs is a singlet almost uncoupled to the Mn spin. We deduce the zero-field fine structure of the excitonic transitions and compare the results with the recently reported photoluminescence spectra.

DOI: 10.1103/PhysRevB.78.195311 PACS number(s): 73.21.La, 71.55.Eq, 71.70.Gm, 75.50.Pp

I. INTRODUCTION

Semiconductor quantum dots (QDs) containing a single localized spin seem promising for possible applications in spintronics and quantum information processing. Mn-doped QDs of II-VI compounds have been extensively studied in recent years. They belong to the family of diluted magnetic semiconductors (DMSs) with well-characterized carrier-ion spin interactions, which are strongly enhanced in QDs due to the confinement of carriers. This leads to the formation of robust exciton magnetic polaron in QDs containing a substantial number of Mn ions.[1–3] The confinement effects seem even more spectacular in QDs containing a single Mn impurity.[4,5] Magnetic circular dichroism (MCD) measurements in Mn-doped colloidal ZnSe nanocrystals (NCs) (Ref. 6) indicated an order-of-magnitude enhancement of the giant Zeeman effect as compared with the bulk DMS of the same Mn concentration. Single-dot photoluminescence (PL) spectroscopy in Mn-doped CdTe/ZnTe self-assembled quantum dots (SAQDs) revealed a zero-field splitting of the exciton line into six bright components,[7] providing a rather direct evidence of the exciton-Mn spin coupling. More recently, a strikingly different zero-field splitting pattern of the PL has been reported[8] in Mn-doped InAs/GaAs QDs, which arises from the difference in the nature of the Mn impurity in II-VI and III-V semiconductors.

A substitutional transition-metal impurity in a II-VI semiconductor is isoelectronic, and the characteristic magnetic and magneto-optical properties of the corresponding DMSs can be simply described in terms of the ionic angular momenta of the *d*-shell and the *sp-d* interactions with the band carriers. On the other hand, such an impurity in a III-V semiconductor is an acceptor, introducing not only the ionic momenta but also a bound hole (h). In particular, the Mn-associated hole ground state in GaAs and InAs is relatively shallow and mostly originates from the host valence band. The binding energies are 112.4 meV (Ref. 9) and 28 meV,[10] respectively. The electronic structure of the Mn_{Ga} impurity in GaAs has been carefully investigated by spectroscopic methods (see Ref. 9 and references therein). The resulting picture is that of a bound hole of effective angular momentum $j=3/2$ subject to an antiferromagnetic interaction $\varepsilon \mathbf{j}\cdot\mathbf{S}$ with the spin $S=5/2$ of the half-filled Mn *d* shell. The ground state, thus, corresponds to the total angular momentum $J=1$, where $\mathbf{J}=\mathbf{j}+\mathbf{S}$, with $\varepsilon \simeq 5$ meV giving the energy levels. A similar picture seems to fit in with the available experimental information on the Mn impurity in InAs. Indeed, the recently discovered ferromagnetism in both (In,Mn)As and (Ga,Mn)As is well explained by the interaction between the Mn spins mediated by delocalized holes.[11] While the search for higher Curie temperatures has stimulated a lot of studies in III-V DMSs and their heterostructures, to our knowledge, no experimental investigation of Mn-doped III-V QDs was reported prior to Ref. 8. This is perhaps related to the difficulty of sample synthesis.

TABLE I. Table of bulk parameters in GaAs and InAs. The central-cell correction parameters (r_0, V_0) that approximately fit the experimental hole BEs: 112.4 meV and 28 meV, respectively. The calculated effective *sp-d* exchange parameters (ε), as well as the exchange energies (E_{ex}) and the total BEs are also shown.

System	γ_1	γ_2	γ_3	ϵ	r_0 (Å)	V_0 (eV)	$\overline{\lvert f(0)\rvert^2}$ (nm^{-3})	ε (meV)	E_{ex} (meV)	Total BE (meV)
GaAs	7.15	2.03	2.96	10.86	2.8	3.1	0.33002	4.9603	26.042	112.67
InAs	19.7	8.4	9.28	15.15	2.8	2.1	0.05482	1.0159	5.334	27.952

Likewise, theoretical studies of Mn-doped QDs have also mostly focused on II-VI compounds.[12–18] A model for the Mn acceptor in bulk GaAs was previously proposed.[19] It is based on the Baldereschi-Lipari effective-mass theory,[20] extended to include a central-cell correction to the impurity potential and the *sp-d* exchange interaction between the Mn ion and the valence-band holes, usually described in terms of the parameter $N_0\beta$. It established a relationship between $N_0\beta$ and the bound hole exchange parameter ε and fully accounted for the experimental data discussed above. This model was adopted by Govorov[21] in a theoretical study of Mn-doped (In,Ga)As/GaAs SAQDs: the confinement potential was treated as a small perturbation leading to a splitting of the ground-state triplet ($J=1$) into a doublet ($J_z=\pm 1$) and a singlet ($J_z=0$). The same picture has been recently used in Ref. 8 for the interpretation of the PL fine structure. Climente *et al.*[22] reported a direct calculation of the hole ground state in a Mn-doped disk-shaped InAs QD based on the Luttinger Hamiltonian and the Coulomb potential. Here we present a more general theoretical study of the electronic structure of Mn-doped GaAs and InAs QDs, which is also based on the Luttinger Hamiltonian, but with different confinement and impurity potentials. Spherical NCs are represented by hard-wall spheres and lens-shaped SAQDs of cylindrical symmetry by a realistic confinement potential:[24] a finite-barrier square well in the growth direction and a parabolic confinement in the base plane. We use the bulk impurity potential with the central-cell correction as deduced in the model of Ref. 19 after extending it here to the case of InAs.

We also present a preliminary study of the lowest two-hole states, which correspond to the excited states for excitonic recombination giving rise to the steady-state PL. The fine structure of the spectrum is calculated and compared with the experimental data.[8]

The paper is organized as follows. In Sec. II we present the theoretical model for the single-hole eigenstates. The results are presented and discussed in Sec. III. The two-hole eigenstates are considered in Sec. IV. The fine structure of the excitonic spectrum in InAs QDs is presented in Sec. V, which includes a discussion of the PL spectra. Finally, we sum up the main results and the concluding remarks in Sec. VI.

II. THEORETICAL MODEL

We consider a single substitutional Mn impurity in a III-V compound semiconductor QD. For simplicity the impurity is assumed to be situated at the center of the QD. A hole is subjected to interactions with the impurity center as well as to the quantum confinement.

A. Hole-impurity interactions

The Mn impurity is an acceptor in the configuration d^5+h, with a bound hole h and the ionic spin $S=5/2$ of the half-filled d shell. The effective attractive potential of the acceptor center for holes can be represented by[19]

$$V_i(\mathbf{r}) = -\frac{e^2}{\epsilon r} - V_0 \exp[-(r/r_0)^2], \tag{1}$$

where, in addition to the long-range Coulomb potential, we include a central-cell correction of the Gaussian form. The phenomenological parameters V_0 and r_0 are determined self-consistently in each compound in order to reproduce the experimental binding energy (BE) in the bulk semiconductor.

The *sp-d* exchange interaction between a band electron (spin $s=\frac{1}{2}$) and the Mn d electrons (total ionic spin $S=\frac{5}{2}$) located at $\mathbf{R}$ can be written as

$$H_{sp-d} = -J(\mathbf{r}-\mathbf{R})\mathbf{s}\cdot\mathbf{S}. \tag{2}$$

It can be treated by the method of perturbation. As shown in Ref. 19, in the ground-state multiplet of the impurity in the bulk semiconductor, calculated within the Luttinger Hamiltonian in the spherical approximation, H_{sp-d} takes the simple isotropic form

$$\hat{H} = \varepsilon \mathbf{j}\cdot\mathbf{S}. \tag{3}$$

Here the effective exchange parameter is given by $\varepsilon = -(\beta/3)\overline{|f(0)|^2}$, a weighted average of the valence-band exchange over the ground-state wave function around the impurity site $\mathbf{R}=0$. A good estimate of the spatial extent of $J(\mathbf{r})$ is the distance d to the second nearest neighbors. Recall that $\beta \equiv \langle X|J(\mathbf{r})|X\rangle$, where $|X\rangle$ is a valence-band orbital Bloch function at $k=0$. Usually, it is measured in terms of $N_0\beta$, where N_0 is the primitive cell density in the crystal. A typical value in Mn-based DMSs is $N_O\beta \sim -1$ eV. This yields an additional contribution to the hole binding energy

$$E_{ex} = -\varepsilon\{J(J+1) - S(S+1) - j(j+1)\} = (21/4)\varepsilon \tag{4}$$

as $J=1$ in the ground state. Clearly, E_{ex} also depends on V_0 and r_0.

We determine V_0 and r_0 which give the best fit to the available experimental data on the Mn impurity in the bulk. This was done previously in Ref. 19 for GaAs. Here the same model is extended to the case of InAs. The results are

explicitly shown in Table I along with the Luttinger parameters (γ's) and dielectric constants (ϵ) from the semiconductor data handbook.[23] Note that we have used ϵ_∞ (ϵ_0) for GaAs (InAs) as the BE is larger (smaller) than the LO phonon energy. The bulk exchange parameter is assumed $N_0\beta = -1$ eV in both compounds.[11,19] In addition to the ground-state energy, the calculated value of $\varepsilon \simeq 5$ meV in GaAs explicitly fits the first excited state, as well as the electron paramagnetic resonance (EPR) data.[9]

B. Confinement potential

Colloidal nanocrystals are typically spherical, and the corresponding confinement potential is modeled as usual by the infinite spherical well: $V_c(r)=0$ for $r \leq a$, and $V_c=\infty$ otherwise. Here a is the NC radius. The Mn-doped NCs can, thus, be treated in the spherical approximation as the bulk impurity problem discussed above with the additional boundary condition: the wave function must vanish at $r=a$. We follow the numerical procedure explained in Appendix A of Ref. 13.

Self-assembled QDs tend to be lens shaped. Pedersen and Chang[24] developed a fairly realistic model of cylindrical symmetry, which we adopt here for treating the impurity problem. It is based on the Luttinger Hamiltonian in the axial approximation discussed below. The confinement potential is assumed parabolic in the x-y plane and a finite square well along the growth direction z with the depth defined by the valence-band offset ΔE_v,

$$V_c(\rho,z) = V_\parallel(z) + V_\perp(\rho),$$

$$V_\parallel(z) = \Delta E_v, \quad |z| \geq w/2,$$

$$= 0, \quad |z| < w/2,$$

$$V_\perp(\rho) = \frac{1}{2}K\rho^2 \tag{5}$$

in cylindrical coordinates. Here K is the force constant of the harmonic oscillator. Note that in the case of strained quantum wells (QWs) the band offset is not the same for the light-hole (lh) and heavy-hole (hh) valence bands.

C. Self-assembled quantum dots

The main focus of our paper is on the hole eigenstates in SAQDs. Here we explain our treatment of the impurity problem in detail. The Hamiltonian of the system is $H=H_0+H_{sp\text{-}d}$, where the "orbital" part

$$H_0 = H_L + V_c(\boldsymbol{r}) + V_i(\boldsymbol{r}). \tag{6}$$

Here H_L is the Luttinger Hamiltonian describing hole kinetic energy in the effective-mass approximation. The other terms, respectively, represent the confinement and impurity potentials described above. Explicitly,[24]

$$H_L = \begin{pmatrix} H_h & R & S & 0 \\ R^* & H_l + \Delta_{lh} & 0 & S \\ S^* & 0 & H_l + \Delta_{lh} & -R \\ 0 & S^* & -R^* & H_h \end{pmatrix}, \tag{7}$$

where

$$H_h = \frac{\hbar^2}{2m_0}[(\gamma_1+\gamma_2)(k_x^2+k_y^2) + (\gamma_1 - 2\gamma_2)k_z^2],$$

$$H_l = \frac{\hbar^2}{2m_0}[(\gamma_1-\gamma_2)(k_x^2+k_y^2) + (\gamma_1 + 2\gamma_2)k_z^2],$$

$$R = \frac{\hbar^2}{2m_0}[2\sqrt{3}\gamma_3 i k_- k_z],$$

$$S = \frac{\hbar^2}{2m_0}[\sqrt{3}\gamma k_-^2 + \sqrt{3}\gamma' k_+^2], \tag{8}$$

with $k_\pm = k_x \pm i k_y$ and $\boldsymbol{k} = -i\nabla$. Here γ_1, γ_2, and γ_3 are the Luttinger parameters, and $\gamma = \frac{1}{2}(\gamma_2+\gamma_3)$ and $\gamma' = \frac{1}{2}(\gamma_2 - \gamma_3)$. Note that the small linear terms in the $\mathbf{k}\cdot\mathbf{p}$ Hamiltonian arising from the lack of inversion symmetry in III-V compounds are neglected. The problem is further simplified by adopting the axial approximation in order to retain cylindrical symmetry about the z axis. It consists in setting $\gamma'=0$, justified by the smallness of the parameter $\delta = \frac{\gamma_3-\gamma_2}{\gamma_1}$ compared to 1 (0.13 in GaAs and 0.044 in InAs) since the warping terms are second order in δ. The shift Δ_{lh} of the light-hole Hamiltonian H_l represents the strain-induced separation between the light- and heavy-hole bands. In lattice-matched GaAs/(Ga,Al)As QDs $\Delta_{lh}=0$. But in strained InAs/GaAs QDs a typical value is $\Delta_{lh} \simeq 200$ meV.[25,26]

The basis of the H_L matrix shown above are the band-edge Bloch functions of the hole: u_μ^h in the order $\mu = 3/2, 1/2, -1/2, -3/2$. Note that the phase convention chosen here is neither that of Luttinger nor that of the standard angular momentum eigenfunctions $|3/2, \mu\rangle$. Explicitly,

$$u_{3/2}^h = -\left|\frac{3}{2},\frac{3}{2}\right\rangle, \quad u_{1/2}^h = i\left|\frac{3}{2},\frac{1}{2}\right\rangle,$$
$$u_{-1/2}^h = \left|\frac{3}{2},-\frac{1}{2}\right\rangle, \quad u_{-3/2}^h = -i\left|\frac{3}{2},-\frac{3}{2}\right\rangle. \tag{9}$$

This choice yields a real Hamiltonian matrix H_0 in the following basis[24] for solving the eigenvalue problem in a variational approach.

The basis functions are

$$\Psi_{nls\nu}(\boldsymbol{r}) = F_{nl}(\rho,\phi) f_s(z) u_\nu^h(\boldsymbol{r}), \tag{10}$$

where the envelope function is a product of the two-dimensional (2D) harmonic-oscillator eigenstate $F_{nl}(\rho,\phi)$ for the heavy hole and the sth subband function $f_s(z)$.

The 2D harmonic-oscillator eigenfunctions are given by

$$F_{n,l}(\rho,\phi) = B_{nl}(i\rho)^{|l|}e^{-\rho^2/2a^2}e^{il\phi}L_n^{|l|}(\rho^2/a^2), \tag{11}$$

where $L_n^{|l|}$ is the generalized Laguerre polynomial and B_{nl} is the normalization constant: $B_{nl}=\sqrt{n!/\pi(n+|l|)!}(1/a)^{|l|+1}$. The lateral confinement radius a_h is related to the force constant and the in-plane heavy-hole effective mass $m_h=m_0/(\gamma_1+\gamma_2)$. When the l-h mixing terms in H_L are neglected, they represent the in-plane eigenstates in undoped QDs.

The subband functions are written as

$$f_s(z) = \sqrt{\frac{2}{W}}\sin\left(\frac{s\pi[z+W/2]}{W}\right). \tag{12}$$

Here W is larger than the actual width w of the square QW. It is chosen to cover the dominant region of wave-function penetration into the barrier. In the case of infinite depth $f_s(z)$ with $W=w$ correspond to the undoped QW eigenstates. Generally, the optimal value of W depends on w, the band offset, and the carrier effective mass.[24]

The hole wave functions in both doped and undoped QDs are obtained in the axial approximation for the valence band. The cylindrical symmetry assures that $j_z=\mu$, the sum of the envelope angular momentum l, and the band-edge value ν is a good quantum number. Thus,

$$\psi_\mu^h(\mathbf{r}) = \sum_{\nu,n,s} C_{n,s,\nu}^{\mu}F_{n,\mu-\nu}(\rho,\phi)f_s(z)u_\nu^h(\mathbf{r}). \tag{13}$$

The different hole eigenstates $|\mu|=1/2,3/2,5/2,\ldots$ are doubly degenerate due to time-reversal symmetry and contain contributions from both hh and lh valence-band states. They are also labeled as S, P, $D,\ldots$, according to the lowest angular momentum terms $l=0,1,2,\ldots$, respectively. Parity is also a good quantum number as the inversion asymmetry terms in the $\mathbf{k}\cdot\mathbf{p}$ Hamiltonian are neglected. For instance, the ground state in undoped QDs is typically $S_{3/2}^+$ of even parity. The variational procedure amounts to progressively increasing the number of basis states in the sum in Eq. (13) in order to achieve convergence of the low-energy eigenvalues of H_0 to the desired level of accuracy.

The sp-d exchange interaction term $H_{sp\text{-}d}$ is next written in the subspace of the low-energy eigenstates of H_0. With the Mn atom at the QD center, only $|\mu|=1/2$ and 3/2 levels of the same parity are coupled by $H_{sp\text{-}d}$, which then takes the simple form[18]

$$\langle\psi_\mu^h|H_{sp\text{-}d}|\psi_\nu^h\rangle = -I_h^{\mu\nu}(\mathbf{j}_{\mu\nu}\cdot\mathbf{S}), \tag{14}$$

with the effective coupling parameters

$$I_h^{\mu\nu} = (\beta/3)[1/(\pi a_h^2)]\sum_{m,s,n,t} C_{m,s,\mu}^{\mu*}C_{n,t,\nu}^{\nu}f_s^*(0)f_t(0), \tag{15}$$

which are readily deduced from the computed eigenstates. Note that the matrices $\boldsymbol{j}$ here refer to the angular momentum $j=3/2$ in the basis shown in Eq. (9). Following Ref. 19, if we take into account the fact that $J(r)$ is a rapidly decreasing function with a finite spatial extension of the order of the second neighbor distance d from the Mn impurity, the corrected exchange parameters are given by

$$\bar{I}_h^{\mu\nu} = \frac{a_h^2}{d^2}(1-e^{-d^2/a_h^2})(\beta/3)[1/(\pi a_h^2)]\sum_{m,s,n,t} C_{m,s,\mu}^{\mu*}C_{n,t,\nu}^{\nu}f_s^*(0)f_t(0)$$
$$\times\frac{1}{2}\left[\frac{W}{(s+t)\pi d}\sin\left(\frac{(s+t)\pi d}{W}\right)\right.$$
$$\left.+\frac{W}{(s-t)\pi d}\sin\left(\frac{(s-t)\pi d}{W}\right)\right]. \tag{16}$$

Limiting our considerations to the lowest two orbital states, by symmetry considerations, usually we have only three independent parameters to calculate: $\bar{I}_h^{3/2,3/2}$, $\bar{I}_h^{3/2,1/2}$, and $\bar{I}_h^{1/2,1/2}$.

The presence of in-plane asymmetry in the real SAQDs can be treated by introducing $\delta\equiv(K_x-K_y)/2$, the difference between the x- and y-direction force constants, giving the additional term in the confinement potential

$$V_c^{\text{asym}} = \frac{1}{2}\delta\rho^2\cos 2\phi. \tag{17}$$

This term breaks the cylindrical symmetry and mixes states with μ differing by 2. For instance,

$$\langle\psi_{1/2}^h|V_c^{\text{asym}}|\psi_{-3/2}^h\rangle = \frac{\pi}{2}\delta\sum_{m,s,n,\alpha} C_{m,s,\alpha}^{1/2*}C_{n,s,\alpha}^{-3/2}B_{m,1/2-\alpha}B_{n,-3/2-\alpha}$$
$$\times\int\rho^3(-i\rho)^{|(1/2)-\alpha|}(i\rho)^{|(3/2)+\alpha|}e^{-\rho^2/a^2}$$
$$\times L_m^{|(1/2)-\alpha|}L_n^{|(3/2)+\alpha|}d\rho \tag{18}$$

Obviously the structural asymmetry by itself cannot lift the Kramer's degeneracy of the hole states, but combined with the sp-d exchange it can raise the degeneracy of levels of the full system.

A different kind of symmetry breaking arises in the case of off-axis Mn impurity. As shown in Ref. 18, it is related to the l-h band mixing in the hole wave function and allows spin-flip terms between the states $|\mu=3/2\rangle$ and $|\nu=-3/2\rangle$. By choosing the x axis to pass through the Mn site, $\phi_0=0$, the effective sp-d Hamiltonian in this subspace can be written in a compact form in terms of the $\tilde{j}=1/2$ pseudospin operators

$$H_h' = -3I_h^{3/2,3/2}\left[\tilde{j}_zS_z+\frac{2}{3}\epsilon(\tilde{j}_xS_x+\tilde{j}_yS_y)\right]. \tag{19}$$

For instance, it will directly lift the degeneracy between the states $|\mu=3/2\rangle|S_z=-1/2\rangle$ and $|\mu=-3/2\rangle|S_z=+1/2\rangle$.

III. SINGLE-HOLE STATES

Here we present and discuss some results for the low-energy hole eigenstates in Mn-doped GaAs and InAs quantum dots. They are based on a numerical diagonalization of the effective-mass Hamiltonian H_0 as explained in Sec. II. The number of basis states is progressively increased in order to reach convergence of the ground-state energy to less than 0.1%. The splittings of the lowest two energy levels arising from the sp-d interaction $H_{sp\text{-}d}$ are finally obtained by diagonalizing it in this four-dimensional subspace. We have

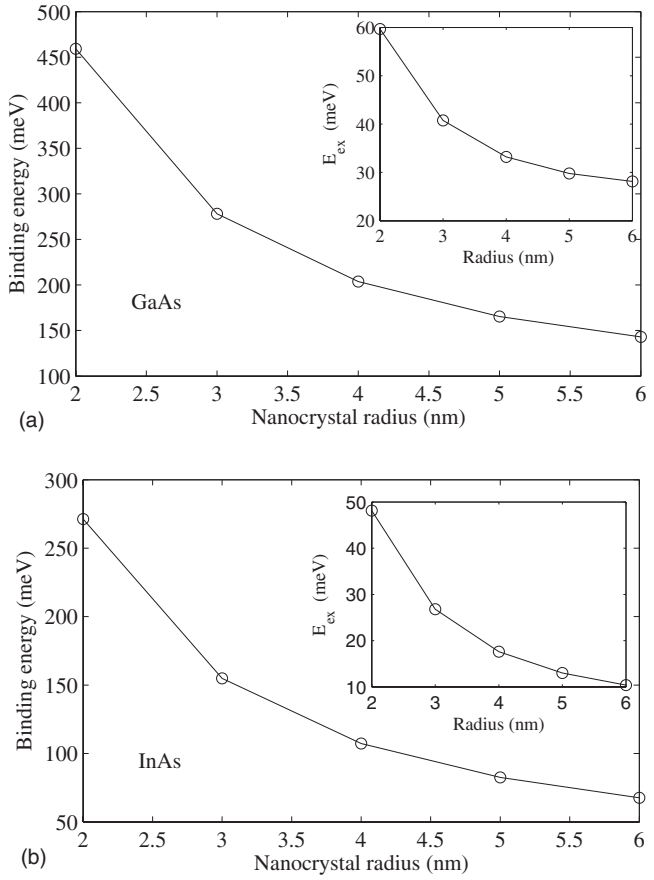

FIG. 1. The hole binding energy (E_B) in spherical nanocrystals is plotted against the radius: The top panel (a) for GaAs and the bottom panel (b) for InAs. The insets show the additional *sp-d* exchange contribution (E_{ex}) to the binding energy.

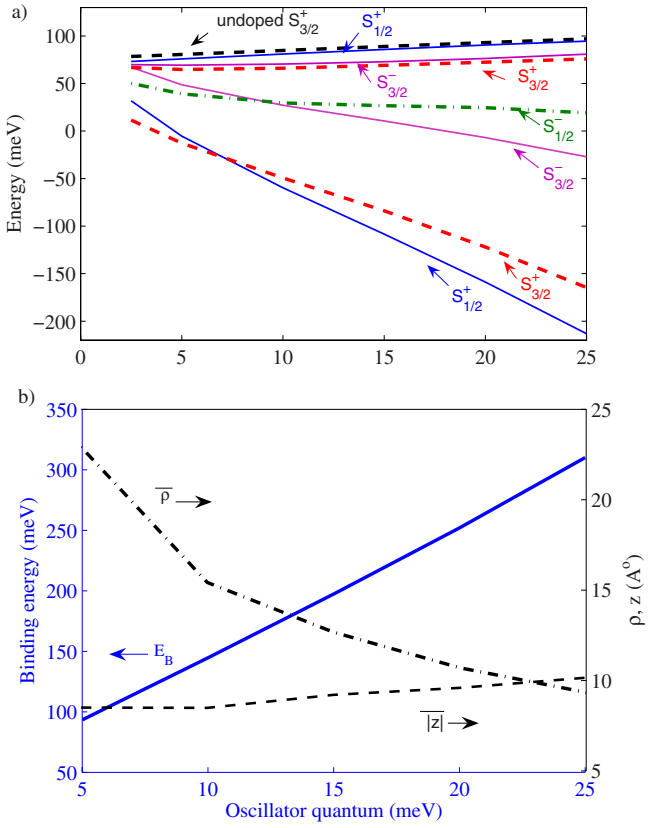

FIG. 2. (Color online) GaAs QD with $w=20$ Å: (a) Eigenvalues versus heavy-hole harmonic-oscillator quantum ($\hbar\omega$). The symmetry classification of the eigenstates is also indicated. The dashed line at the top corresponds to the ground state in the undoped QD. (b) The hole binding energy (E_B), average in-plane radius ($\bar{\rho}$), and average width ($\overline{|z|}$) versus $\hbar\omega$.

also calculated the hole spectrum in the undoped QDs for reference; let us recall that the solution is analytical in the case of spherical NCs.[27] The binding energy is defined as the energy difference between the hole ground states in the undoped and doped QD of the same size,

$$E_B \equiv E_0^{\text{undoped}} - E_0^{\text{doped}}. \tag{20}$$

In spherical NCs, like in the bulk semiconductor, the ground state is always a $j=3/2$-like Γ_8 state with $1S_{3/2}$ envelope function in the spherical approximation. Figure 1 shows the binding energy E_B as a function of the NC radius. In both compounds the BE decreases rather rapidly with increasing size and, in the asymptotic limit, tends to the experimental value in the bulk. However, the approach to the asymptotic limit is somewhat faster in GaAs than in InAs because the bulk Bohr radius is much smaller in the former. Note that the confinement-induced increase in the BE is in accord with the known results for nonmagnetic acceptor or donor impurities in NCs (see Ref. 28 and references therein). The size dependence of the *sp-d* exchange contribution to the BE is shown in the inset. It increases with decreasing size as the hole density around the Mn site (NC center) increases.

While in spherical NCs the size is simply characterized by the radius, the situation is less precise in lens-shaped SAQDs. Typically, the height and the lateral radius, not to speak of the real alloy composition, are indicated only approximately. In the present model of cylindrical symmetry, the QW width w corresponds to the QD height. On the other hand, the in-plane confinement potential is related to the heavy-hole harmonic-oscillator quantum $\hbar\omega=\sqrt{K/m_h}$ and radius $a_h=\sqrt{\hbar/m_h\omega}$. The latter can be considered as an indicator of the lateral size of the QD. Thus, we compute the results for different values of w and $\hbar\omega$. GaAs and InAs QDs are discussed separately. The former refers to the lattice-matched heterostructure GaAs/(Ga,Al)As with $\Delta_{lh}=0$, while the latter corresponds to the strained structure InAs/GaAs with an estimated value of Δ_{lh} between 150 meV (Ref. 29) and 200 meV (Refs. 25 and 26). We have considered three different values of Δ_{lh} from 100 to 200 meV. The Mn impurity input parameters used are those shown in Table I.

A. Self-assembled quantum dots of GaAs

The eigenstates of H_0 in Mn-doped GaAs SAQDs are presented in Fig. 2. The valence-band offset was assumed to be $\Delta E_v=130$ meV after Ref. 24. Panel (a) shows a plot of the energy of the low-lying states against the harmonic-oscillator quantum $\hbar\omega$. The symmetry classification of the eigenstates is also indicated. Panel (b) shows the ground-

TABLE II. GaAs QD with $\hbar\omega=10$ meV: The energy of the lowest levels in meV as a function of the QD height w. The number in the parenthesis distinguishes different levels of the same symmetry. The second column indicates the values of W used for calculating the subband functions.

w (Å)	W (Å)	$S^{+}_{1/2}(1)$	$S^{+}_{3/2}(1)$	$S^{-}_{3/2}(1)$	$S^{-}_{1/2}(1)$	$S^{+}_{1/2}(2)$	$S^{-}_{1/2}(2)$	$S^{+}_{1/2}(2)$
20	56.3	−59.7203	−49.2832	27.1922	29.5738	66.0638	70.4258	81.0346
30	66.3	−88.9240	−76.4391	−6.7402	3.9608	39.0239	41.8339	51.9484
40	76.3	−110.4628	−99.1845	−40.4512	−14.7795	24.1145	24.5229	34.7974

state binding energy (E_B), the average in-plane radius $\bar{\rho}$, and the average width $\bar{|z|}$ against $\hbar\omega$. Table II shows the eigenvalues as functions of the QD height (QW width) w.

The most striking feature of Fig. 2(a) is the confinement-induced crossover of the ground-state symmetry from $S^{+}_{3/2}$ to $S^{+}_{1/2}$ at $\hbar\omega\simeq 7$ meV. The crossover in undoped QDs takes place at much higher values of $\hbar\omega$. For instance, in QDs of height $w=10$ nm the threshold value is 37.7 meV (Ref. 24). The crossover basically corresponds to the change from a dominantly heavy-hole-like state to a light-hole-like one. This is explicitly seen through an analysis of the wave function in terms of the weight factors of the different band states, $W^{\mu}_{\nu}\equiv|\langle\psi^{h}_{\mu}|u^{h}_{\nu}\rangle|^2$, which are shown in Table III. Note how the fraction of the heavy-hole band ($u^{h}_{\pm 3/2}$) changes from 87% to 17% as $\hbar\omega$ goes from 6.5 to 7 meV. The crossover also shows in the variation in $\bar{\rho}$ and $\bar{|z|}$ of Fig. 2(b). In particular, the increase in $\bar{|z|}$ results from the smaller light-hole effective mass along z. The crossover can be explained as follows. The confinement along z first raises the light-hole band above the heavy-hole one. As the lateral confinement is switched on, the in-plane effective mass comes into play. In contrast to the z direction, the in-plane effective mass of the light-hole band is larger, and thus, its energy decreases while that of the heavy-hole band increases with increasing in-plane confinement, giving rise to the crossover. In Mn-doped QDs the impurity potential drastically enhances the confinement and, thus, brings down the threshold of $\hbar\omega$ to much lower values. The effects of varying the QD height on the electronic structure are illustrated in Table II. Although the evolution of the energy levels with w looks rather monotonous, the binding energy (not shown) decreases with increasing w. Also, as w increases, the initial shift at $\hbar\omega=0$ between the light- and heavy-hole bands decreases and the $S^{+}_{3/2}$ to $S^{+}_{1/2}$ crossover moves to a lower $\hbar\omega$. For instance, at $w=4$ nm we find a threshold value of 4.5 meV.

The level splittings arising from the sp-d exchange interaction are presented in Fig. 3. The effective exchange parameters $\bar{I}^{\mu\nu}_{h}$ that concern the lowest two energy levels $S^{+}_{\pm 3/2}$ and $S^{+}_{\pm 1/2}$ are shown in Table III along with the weight factors. The level scheme of the components shown in panel (a) of Fig. 3 was deduced by diagonalizing $H_{sp\text{-}d}$ in the subspace of these two orbital states by using Eq. (14). The component levels are no longer the eigenstates of the total angular momentum $\boldsymbol{J}=\boldsymbol{j}+\boldsymbol{S}$ as in spherical symmetry (bulk or NC). Here, the good quantum number is J_z. We find that the lowest level changes from $J_z=\pm 1$ to $J_z=0$ around the confinement-induced crossover at ~ 7 meV seen in panel (a) of Fig. 2. The level ordering (from below) in the typical QD size range ($\hbar\omega\geq 10$ meV) is $J_z=0, \pm 1, \pm 2, \ldots$. It clearly contradicts the predicted level scheme in the perturbative picture.[21] Panel (b) of Fig. 3 shows the exchange contribution E_{ex} to the binding energy as a function of $\hbar\omega$. The jump at the crossover is quite remarkable. It arises from the enhanced interaction between the two levels, $S^{+}_{\pm 3/2}$ and $S^{+}_{\pm 1/2}$, at the crossing point, as illustrated in panel (a). Anyway, the effective exchange parameters and E_{ex} are more than an order of magnitude smaller than in the bulk because the wave function is more spread out laterally in the anisotropic SAQDs, as discussed below. This also invalidates the previous assumption of unmodified exchange parameter ε.[21]

B. Self-assembled quantum dots of InAs

We next present analogous results for InAs/GaAs QDs. Note that the band offsets for the heavy- and light-hole components in the Luttinger Hamiltonian are different and de-

TABLE III. GaAs QD with $w=20$ Å: The ground-state (g) weight factors versus $\hbar\omega$. The effective sp-d exchange parameters (in meV) for the lowest two levels are also shown. Note that $g=3/2$ for $\hbar\omega\leq 6.5$ meV and $g=1/2$ for $\hbar\omega\geq 7$ meV.

$\hbar\omega$	$W^{g}_{3/2}$	$W^{g}_{1/2}$	$W^{g}_{-1/2}$	$W^{g}_{-3/2}$	$\bar{I}^{3/2,3/2}$	$\bar{I}^{1/2,1/2}$	$\bar{I}^{3/2,1/2}$
5	0.8704	0.0185	0.1058	0.0054	−0.1620	−0.1988	−0.1796
6.5	0.8607	0.0185	0.1152	0.0055	−0.1987	−0.2540	0.2249
7	0.0590	0.8273	0.0021	0.1116	−0.2098	−0.2716	0.2391
10	0.0502	0.8445	0.0017	0.1036	−0.2530	−0.3623	0.3039
15	0.0362	0.8664	0.0013	0.0961	−0.3188	−0.4800	−0.3935
20	0.0259	0.8816	0.0011	0.0915	−0.3256	−0.5361	−0.4227
25	0.0194	0.8919	0.0010	0.0877	−0.2992	−0.5421	0.4113

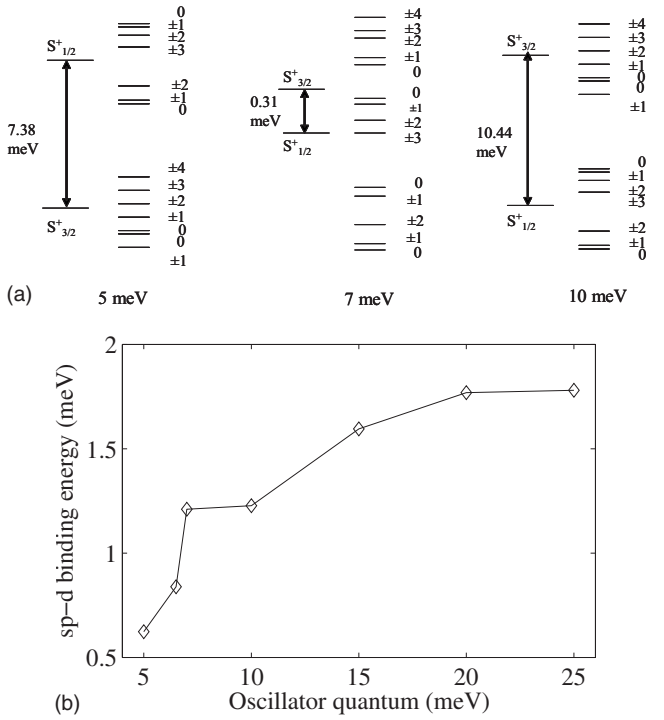

FIG. 3. GaAs QD with $w=20$ Å: The *sp-d* exchange contribution to the binding energy as a function of the oscillator quantum. A schematic representation of the exchange splitting of the lowest two energy levels at three interesting $\hbar\omega$ values is shown in the top panel.

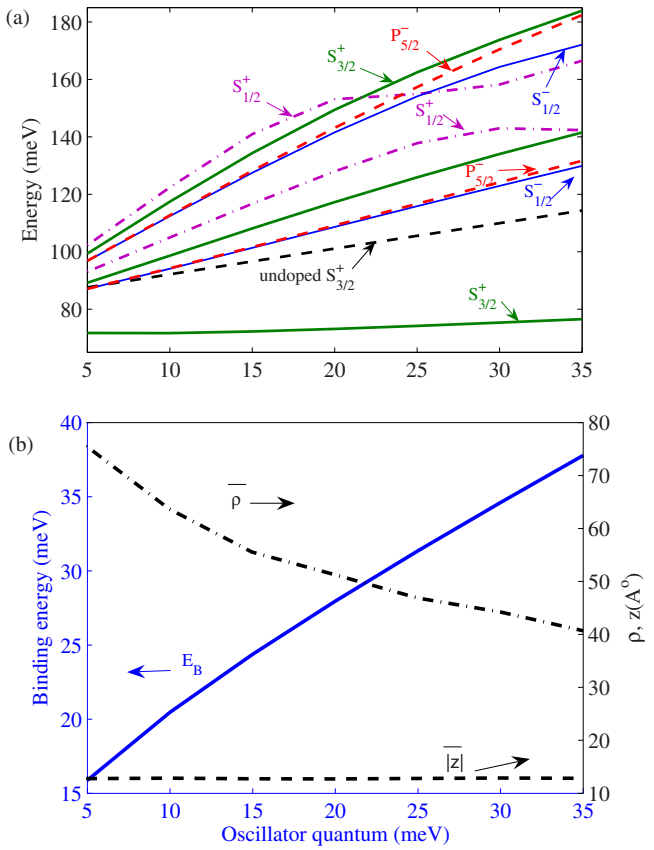

FIG. 4. (Color online) InAs QD with $w=25$ Å and $\Delta_{lh}=200$ meV: (a) Eigenvalues versus oscillator quantum ($\hbar\omega$). (b) The hole binding energy (E_B), average in-plane radius ($\bar{\rho}$), and average width ($\overline{|z|}$) versus $\hbar\omega$.

pend on the value of Δ_{lh}. We have assumed the heavy-hole value $\Delta E_v=350$ meV in this system following the energy level diagram in Ref. 25. In Fig. 4 panel (a) shows the low-lying energy levels plotted against $\hbar\omega$.

Note that in contrast with GaAs QDs, there is no crossover in the ground state although a level crossing does occur at higher energy. This is related to the fact that the light-hole subband is pushed up so much by the built-in strain that it hardly contributes to the ground state even in the doped QD. The ground-state binding energy (E_B), average radius $\bar{\rho}$, and width $\overline{|z|}$ are shown in panel (b). The effects of the QD height w and the light- and heavy-hole separation Δ_{lh} are illustrated in Table IV.

Note that the ground state is an even parity $S^+_{3/2}$ throughout, which is also the symmetry of the ground state in the undoped QD represented by the dashed line in panel (a). But the first excited state is nearly degenerate; the level $S^-_{1/2}$ lying barely below $P^-_{5/2}$, both of odd parity. They basically arise from the $l=\pm 1$ orbital angular momentum eigenstates of the in-plane harmonic oscillator coupled to the *hh* "spin" $\nu=\pm 3/2$, while the ground state belongs to $l=0$. Indeed the first excitation energy is of the order of $\hbar\omega$. As can be seen in Table IV, the splitting between the states $S^-_{1/2}$ and $P^-_{5/2}$ increases with decreasing Δ_{lh} due to an increasing contribution from the light-hole band states. Also, there is a crossover between the second $S^+_{3/2}$ and the first $S^+_{1/2}$ states.

A feature in Fig. 4(b) that appears anomalous at first sight is that E_B in the low-confinement region is lower than that in the bulk ($\simeq 22$ meV from Table I). In an undoped SAQD the localization of the carrier in the z direction is controlled by the band offset and the longitudinal effective mass. It is only weakly affected by the Coulomb potential of the acceptor center, which essentially localizes the in-plane motion. But the in-plane heavy-hole effective mass is much smaller than the three-dimensional (3D) heavy-hole effective mass, which determines the binding energy in the bulk. This is in accord with the much larger in-plane radial extension of the hole orbit in the QD as explicitly shown in Fig. 5, which presents a comparison of the spatial distribution in the ground state between a relatively large-size SAQD and the bulk semiconductor.

The difference of parity between the lowest two states in InAs QDs has an interesting consequence: the levels $S^+_{3/2}$ and $S^-_{1/2}$ are not coupled by $H_{sp\text{-}d}$. Moreover, it can be shown that the effective exchange parameter $\bar{I}_h^{1/2,1/2}$ in the upper level vanishes by symmetry for the on-center Mn. We, thus, obtain two well-separated levels, with only the lower one $S^+_{3/2}$ split into six doublets, with small splittings controlled by the effective exchange parameter $\bar{I}_h^{3/2,3/2}$.

The values of the exchange parameter and the ground-state weight factors are shown in Table V. The lower set of levels is given by $-15/4,-9/4,-3/4,3/4,9/4,15/4$ in units of $\mathcal{I}\equiv-\bar{I}_h^{3/2,3/2}$. The respective eigenstates are the doublets: $|j_z=\pm 3/2\rangle|S_z=\mp 5/2\rangle$, $|\pm 3/2\rangle|\mp 3/2\rangle$, $|\pm 3/2\rangle|\mp 1/2\rangle$, $|\pm 3/2\rangle|\pm 1/2\rangle$, $|\pm 3/2\rangle|\pm 3/2\rangle$, and $|\pm 3/2\rangle|\pm 5/2\rangle$, which

TABLE IV. InAs QD with $\hbar\omega=30$ meV: The lowest energy levels in meV as functions of the QD height w and the strain-induced l-h band splitting Δ_{lh}.

Δ_{lh} (meV)	w (Å)	$S^{+}_{3/2}(1)$	$S^{-}_{1/2}(1)$	$P^{-}_{5/2}(1)$	$S^{+}_{3/2}(2)$	$S^{+}_{1/2}(1)$	$S^{+}_{1/2}(2)$
200	40	35.7722	81.9968	83.2736	94.2945	102.9772	119.7358
200	30	57.2696	104.2855	105.5187	115.9803	125.2459	140.9305
200	25	75.3336	122.9498	124.1940	134.0307	142.9771	158.2402
150	25	73.5685	121.7204	123.3841	130.0035	123.8749	151.5541
100	25	71.0902	119.3572	122.5208	123.6322	99.2654	148.2897

respectively correspond to $J_z=j_z+S_z=\pm1,0,\pm1,\pm2,\pm3,\pm4$. Notice that the $J_z=0$ level is also doubly degenerate. While the identification of the ground state does coincide with that in the perturbative picture,[21] the overall level scheme, as well as the binding energy contribution $E_{\mathrm{ex}}=(15/4)\mathcal{I}$, is dramatically different. $\mathcal{I}$ is indeed an order of magnitude smaller than the bulk exchange parameter ε, similar to that in GaAs QDs.

Also, in contrast with the model of Ref. 21, the double degeneracy of the ground-state $J_z=\pm1$ in the present model can be raised only by the combined effects of structural asymmetry and off-axis impurity site at a relatively high order of perturbation.

IV. TWO-HOLE STATES

As the Mn-doped III-V compound QD contains a resident hole, two-hole states come up in most experimental situations. The second hole can be introduced via optical excitation or electrical injection. For instance, in steady-state PL experiments, the excited state of the recombination is the lowest state of the system consisting of two holes and one electron. Here we present a preliminary discussion of the two-hole eigenvalue problem.

The Hamiltonian for two holes in a QD containing a substitutional Mn impurity at the center is given by

$$H_{12}(\boldsymbol{r_1},s_1,\boldsymbol{r_2},s_2)=H(\boldsymbol{r_1},\boldsymbol{s_1})+H(\boldsymbol{r_2},\boldsymbol{s_2})+V_{12}(\boldsymbol{r_1},\boldsymbol{r_2}), \quad (21)$$

where $V_{12}(\boldsymbol{r_1},\boldsymbol{r_2})=e^2/(\epsilon_0|\boldsymbol{r_1}-\boldsymbol{r_2}|)$ is Coulomb repulsion between the holes and $H(\boldsymbol{r},\boldsymbol{s})\equiv H_0+H_{sp\text{-}d}$. As the Hamiltonian retains the cylindrical symmetry, once again, the eigenvalues can be classified according to the z component of the total angular momentum $j^{(2)}_z=j_{1z}+j_{2z}$ and the parity.

The antisymmetrized products of single-hole eigenstates

$$|\mu,\nu\rangle^P\equiv\frac{1}{\sqrt{2}}[\psi^p_\mu(\boldsymbol{r_1})\psi^q_\nu(\boldsymbol{r_2})-\psi^p_\mu(\boldsymbol{r_2})\psi^q_\nu(\boldsymbol{r_1})] \quad (22)$$

of a given $j^{(2)}_z=m^{(2)}=\mu+\nu$ and parity P can be used as a basis set for computing the two-hole eigenstates of the same symmetry. Note that here we have replaced the superscript h in the single-hole eigenfunctions by the respective parity indices p and q; they determine the parity P of the product function.

In order to obtain an accurate estimation of the low-energy two-hole states, a configuration interaction approach is generally necessary. However, when the spacing Δ between the lowest single-particle states is large compared to the Coulomb integral J, a perturbative treatment turns out to be adequate for obtaining satisfactory results. Considering the single-hole spectra discussed in Sec. III, it is clear that we cannot apply this perturbation approach in the case of GaAs QDs, where the low-energy single-hole states are rather close to one another, in particular, in the crossover region. On the other hand, even though $\Delta\sim J$, the two-hole ground state in undoped InAs QDs was found to be a singlet in accord with the Aufbau principle.[30] This means that the dominant term in the two-hole ground state $|\mathcal{S}^{+}_0\rangle$ is given by the full occupation of the single-hole ground-state doublet. The first two-hole excited state $|\mathcal{S}^{-}_1\rangle$ would then correspond to a single occupation of the lowest two one-hole levels. We

TABLE V. InAs QD with $w=25$ Å: Ground-state ($g=3/2$) weight factors and exchange parameter $\bar{I}^{3/2,3/2}_h$ (in meV) for different values of $\hbar\omega$ and Δ_{lh}.

$\hbar\omega$	Δ_{lh}	$W^g_{3/2}$	$W^g_{1/2}$	$W^g_{-1/2}$	$W^g_{-3/2}$	$\bar{I}^{3/2,3/2}$
5	200	0.9927	0.0031	0.0040	0.0002	−0.0162
10	200	0.9866	0.0042	0.0087	0.0005	−0.0262
15	200	0.9803	0.0051	0.0138	0.0008	−0.0362
20	200	0.9738	0.0059	0.0191	0.0012	−0.0465
25	200	0.9673	0.0067	0.0246	0.0015	−0.0571
30	200	0.9607	0.0074	0.0302	0.0018	−0.0679
30	150	0.9448	0.0077	0.0437	0.0038	−0.0872
30	100	0.9143	0.0082	0.0696	0.0079	−0.1132

TABLE VI. InAs QD with $w=25$ Å and $\Delta_{lh}=200$ meV: The lowest two single-hole eigenvalues, the two-hole direct and exchange Coulomb integrals between these states, and finally the approximate energy of the two lowest two-hole states; all the entries are in meV.

$\hbar\omega$	$S^+_{3/2}$	$S^-_{1/2}$	$J_{3/2,-3/2}$	$J_{3/2,-1/2}$	$K_{3/2,-3/2}$	$K_{3/2,-1/2}$	$\mathcal{S}^+_0$	$\mathcal{S}^-_1$
5	71.7422	87.0482	12.3222	5.2437	3.0517×10^{-6}	3.387×10^{-8}	155.8066	164.0341
10	71.6764	94.0793	14.6425	6.9180	3.2392×10^{-4}	2.0363×10^{-6}	157.9950	172.6737
15	72.2600	101.3368	15.8252	8.6165	0.0047	0.0021	160.3405	182.2112
20	73.1398	108.6243	17.7564	9.7903	0.0993	0.0297	163.9367	191.5247
25	74.1867	115.8492	18.0872	10.7631	0.5893	0.5569	165.8713	200.2421
30	75.3336	122.9498	19.2342	11.7635	1.7535	1.2119	168.1479	208.8350
35	76.5452	129.8766	19.4583	12.5342	2.0315	1.5030	170.5172	217.4530

shall apply this approximation in Mn-doped InAs QDs. Thus,

$$|\mathcal{S}^+_0\rangle \simeq |S^+_{3/2},S^+_{-3/2}\rangle = \frac{1}{\sqrt{2}}[|S^+_{3/2}(\boldsymbol{r_1})\rangle|S^+_{-3/2}(\boldsymbol{r_2})\rangle - |S^+_{-3/2}(\boldsymbol{r_1})\rangle|S^+_{3/2}(\boldsymbol{r_2})\rangle], \tag{23}$$

$$|\mathcal{S}^-_1\rangle \simeq |S^+_{3/2},S^-_{-1/2}\rangle = \frac{1}{\sqrt{2}}[|S^+_{3/2}(\boldsymbol{r_1})\rangle|S^-_{-1/2}(\boldsymbol{r_2})\rangle - |S^-_{-1/2}(\boldsymbol{r_1})\rangle|S^+_{3/2}(\boldsymbol{r_2})\rangle], \tag{24}$$

with the respective energy expectation values

$$E^{(2)}_0 = \langle\mathcal{S}^+_0|H_{12}(\boldsymbol{r_1},\boldsymbol{r_2})|\mathcal{S}^+_0\rangle = 2E_{S^+_{3/2}} + J_{3/2,-3/2} - K_{3/2,-3/2}, \tag{25}$$

$$E^{(2)}_1 = \langle\mathcal{S}^-_1|H_{12}(\boldsymbol{r_1},\boldsymbol{r_2})|\mathcal{S}^-_1\rangle = E_{S^+_{3/2}} + E_{S^-_{1/2}} + J_{3/2,-1/2} - K_{3/2,-1/2}, \tag{26}$$

where $J_{i,j}$ and $K_{i,j}$ are the direct and exchange Coulomb integrals, respectively, defined as usual. We calculate them numerically from our one-hole eigenvectors. The results are shown in Table VI.

Notice that the exchange integrals K_{ij} are negligibly small. This is because the orthogonal heavy-hole spin states 3/2 and $-3/2$, respectively, dominate the two eigenstates concerned as the light-hole band mixing is almost negligible in this system. From Table VI we see that the ground state is a singlet, and the first excitation energy $\Delta E^{(2)} \equiv E^{(2)}_1 - E^{(2)}_0$ increases from about 8 to 47 meV as the in-plane confinement increases from $\hbar\omega=5$ to 35 meV. While the singlet character of the ground state is in agreement with Climente *et al.*,[22] their estimated value of 200 meV for the excitation energy is much larger than the values obtained here.

Let us now consider the effects of the *sp-d* exchange on the two-hole states. Following Eq. (14), the relevant matrix elements of

$$H^{(2)}_{sp-d} = -J(\boldsymbol{r}_1)\boldsymbol{s}_1\cdot\boldsymbol{S} - J(\boldsymbol{r}_2)\boldsymbol{s}_2\cdot\boldsymbol{S} \tag{27}$$

in the product space can be written in the compact form

$$\langle\mu,\nu|H^{(2)}_{sp-d}|\mu',\nu'\rangle = \langle\mu,\nu| - (\boldsymbol{k}_1+\boldsymbol{k}_2)\cdot\boldsymbol{S}|\mu',\nu'\rangle, \tag{28}$$

where $\langle\mu|\boldsymbol{k}_i|\nu\rangle \equiv I^{\mu\nu}_h(\boldsymbol{j}_i)_{\mu\nu}$.

As the lowest two energy levels in InAs QDs, $E^{(2)}_0$ and $E^{(2)}_1$, belong to opposite parities, they are not coupled by $H^{(2)}_{sp-d}$. Also, it follows from Eqs. (23) and (28) that $\langle\mathcal{S}^+_0|H^{(2)}_{sp-d}|\mathcal{S}^+_0\rangle \simeq 0$. Thus, in the present approximation, the singlet ground state remains unaffected by the *sp-d* interaction. On the other hand, the first excited state is a doublet $\{|\mathcal{S}^-_1\rangle,|\mathcal{S}^-_{-1}\rangle\}$, which is split by the *sp-d* exchange. As $H^{(2)}_{sp-d}$ has no off-diagonal element in the corresponding 2×2 matrix and $\bar{I}^{1/2,1/2}_h=0$, the two components $j^{(2)}_z=\pm1$ are given by

$$\Delta E^{(2)}_{\pm1} = \pm\frac{3}{2}\bar{I}^{3/2,3/2}_h S_z. \tag{29}$$

V. EXCITONIC SPECTRUM

We shall now discuss the fundamental optical transitions in a Mn-doped QD, limiting ourselves to the case of InAs. They involve electric dipole matrix elements between a one-hole ground-state multiplet $|i\rangle \equiv |\mu=\pm3/2\rangle|S=5/2,S_z=M_S\rangle$ and the lowest manifold of the system consisting of two holes and one electron. As the lowest two-hole state is a singlet, the exchange interaction between the two holes and the electron can be neglected. As the energy gap concerned is much larger than the *e-h* Coulomb interaction, the latter can be treated as a perturbation, giving rise to a shift in the optical gap. Thus, the excited-state manifold of the optical transition can be written as $|f\rangle \equiv |\mathcal{S}^+_0\rangle|\Sigma,M\rangle$, where $|\Sigma,M\rangle$ denote the eigenstates of the electron-Mn *sp-d* exchange Hamiltonian H_e deduced below.

In the present model of QD the electron wave functions in the effective-mass approximation can be written as

$$\psi^e_{n,l,t,m}(\mathbf{r}) = f^e_t(z)F^e_{n,l}(\rho,\phi)u^c_m(\mathbf{r}), \tag{30}$$

where $f^e_t(z)$ is the subband envelope function and u^c_m is the conduction band-edge periodic Bloch function of spin $s_z=m=\pm\frac{1}{2}$. As the QW confinement effect on the electron is very strong, the energy levels are well separated. Accurate infrared spectroscopy in InAs/GaAs QDs yields a separation of ~60 meV (see Ref. 25 and references therein), which suggests this value of $\hbar\omega_e$ in our model. For the excited states of the optical transitions under consideration, we need only the electron ground-state spin doublets: $n=0$, $l=0$, $t=1$, and $m=\pm1/2$. It is easy to see that the *sp-d* exchange

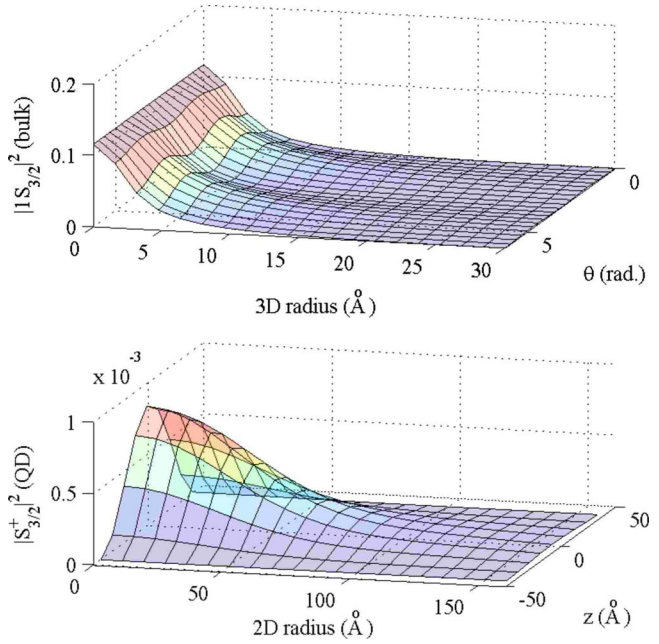

FIG. 5. (Color online) Comparison of the bulk and the quantum dot ground-state wave functions in InAs: $|\psi^h(\boldsymbol{r})|^2$ against the spatial coordinates. Here for the quantum dot $\hbar\omega=5$ meV and $w=25$ Å.

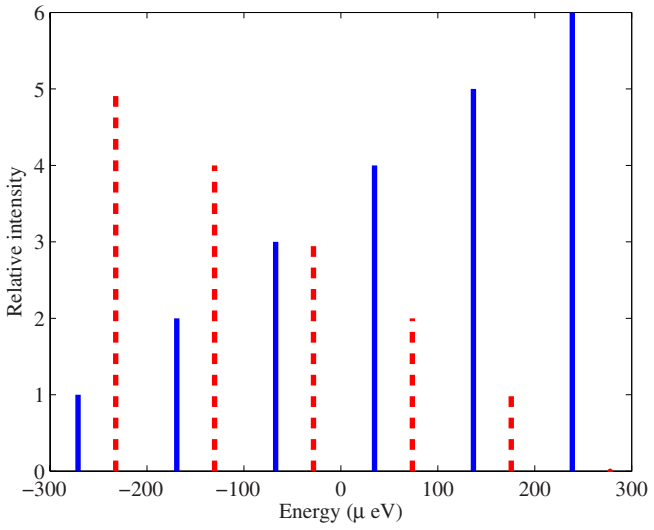

FIG. 6. (Color online) InAs QDs with the effective *sp-d* exchange parameters $I_e=13$ μeV and $\bar{I}_h^{3/2,3/2}=-68$ μeV: Relative oscillator strength versus energy of the zero-field excitonic components. The zero of energy is at the excitonic transition in the absence of *sp-d* exchange.

Hamiltonian in this subspace retains the isotropic form: $H_e=-I_e\mathbf{s}\cdot\mathbf{S}$, independently of the Mn position. Here $I_e=[\alpha/(\pi a_e^2)]\exp(-\rho_0^2/a_e^2)|f_1^e(z_0)|^2$, where $\mathbf{R}=(z_0,\rho_0,\phi_0)$ is the Mn site. The measured value of the bulk exchange parameter $N_0\alpha$ in II-VI DMSs is typically about 0.2 eV. Following the level scheme in Ref. 25, the electron ground-state energy referred to the bottom of the conduction band is ~296 meV, which represents the sum $\hbar\omega_e+(\hbar k_0)^2/(2m_e)$ in our model, the second term being the QW confinement energy. With the QD height $w=2.5$ nm, we thus obtain $I_e\simeq 13$ μeV for an on-center impurity.

The electron-Mn spin Hamiltonian H_e is easily diagonalized: the eigenstates $|\Sigma,M\rangle$ are those of the total spin $\boldsymbol{\Sigma}=\boldsymbol{S}+\boldsymbol{s}$,

$$|3,M\rangle=\sqrt{\frac{3+M}{6}}\left|\frac{5}{2},M-\frac{1}{2}\right\rangle\left|\frac{1}{2},\frac{1}{2}\right\rangle+\sqrt{\frac{3-M}{6}}\left|\frac{5}{2},M+\frac{1}{2}\right\rangle\left|\frac{1}{2},-\frac{1}{2}\right\rangle,$$

$$|2,M\rangle=-\sqrt{\frac{3-M}{6}}\left|\frac{5}{2},M-\frac{1}{2}\right\rangle\left|\frac{1}{2},\frac{1}{2}\right\rangle+\sqrt{\frac{3+M}{6}}\left|\frac{5}{2},M+\frac{1}{2}\right\rangle\left|\frac{1}{2},-\frac{1}{2}\right\rangle. \quad (31)$$

Also the two eigenvalues are $E^e_\Sigma=-I_e[\Sigma(\Sigma+1)-(35/4)-(3/4)]$. Recalling that we have six energy levels of the hole-Mn system, *a priori* there should be 12 zero-field components in the excitonic spectrum.

The oscillator strength of the electric dipole transition that creates (absorption) or annihilates (recombination) an electron (ψ^e_m) and a hole (ψ^h_μ) is proportional to $|P^\eta_{m,\mu}|^2$, where η is the polarization of light and the momentum matrix element $P^\eta_{m,\mu}\equiv\langle\psi^e_m|\boldsymbol{P}\cdot\boldsymbol{\eta}|\psi^v_{-\mu}\rangle$. Here the "valence-band" electron wave function $\psi^v_{-\mu}$ is the time-reversed version of ψ^h_μ. Setting $\eta=\pm$ for the circular polarization $\sigma_\pm$, we obtain for the allowed transitions: $P^+_{-1/2,3/2}=P^-_{1/2,-3/2}=\mathcal{J}\langle S|P_x|X\rangle$, where S is the s-like orbital part of u^c_m, X is the p-like one of u^v_μ, and $\mathcal{J}=\Sigma C^{3/2}_{n,s,3/2}\int f_1^e(z)f_s(z)dz\int F^e_{00}(\rho)F_{n0}(\rho)\rho d\rho$ is the envelope overlap integral. Thus, the momentum matrix element for the allowed interband transitions in the present subspace is a constant. Moreover, the relative oscillator strengths of the transitions between the set of six hole-Mn sublevels $|i\rangle=|\mu=\pm 3/2\rangle|S=5/2,S_z=M_S\rangle$ and the two $(2h+1e)$-Mn sublevels $|f\rangle=|\mathcal{S}^+_0\rangle|\Sigma,M\rangle$ are given by $R^\pm_{if}=|\langle m=\mp\frac{1}{2},M_S|\Sigma,M\rangle|^2$. A plot of these numbers is shown in Fig. 6, where the solid (broken) bars correspond to the lower (higher) electron level $\Sigma=3$ ($\Sigma=2$). We have assumed $I_e=13$ μeV and $\bar{I}_h^{3/2,3/2}=-68$ μeV based on our theoretical estimates for InAs QDs with $w=25$ Å, $\Delta_{lh}=200$ meV, and $\hbar\omega=30$ meV, which correspond to the level scheme in Ref. 25.

Clearly, the zero-field splitting pattern of the fundamental absorption or emission line in InAS QDs presented in Fig. 6 as such does not fit in with the experimental PL spectrum reported by Kudelski *et al.*[8] However, the phenomenological spin Hamiltonian model used in Ref. 8 for interpretation of the data is based on the assumption of a photoinjected QD exciton weakly interacting with a bulklike hole-Mn impurity complex, which cannot be justified. We have shown that the picture of a weakly perturbed impurity complex[21] is incompatible with our results: the anisotropic confinement in SAQDs drastically modifies the impurity level scheme. Moreover, the phenomenological model distinguishes the QD holes from the impurity-bound holes, which are essentially indistinguishable particles, both subjected to the same confinement and impurity potentials. The steady-state PL

presumably originates from the lowest states of the system $(2h+1e)$-Mn after energy relaxation of the optically injected electron-hole pair. Our treatment of this system based on a perturbative approach for the hole-hole interaction is admittedly an approximation. While it seems reasonable in InAs/GaAs QDs with $\Delta_{lh} \sim 200$ meV in the high-confinement size range ($\hbar\omega \geq 30$ meV), its validity is doubtful in the low-confinement region ($\hbar\omega \leq 10$ meV), even more so if any composition fluctuation lowers the local Δ_{lh} value around the Mn site. A full configuration interaction calculation is in progress and will be reported elsewhere. At this point, it seems a singlet two-hole ground state in Mn-doped InAs QDs, obtained here as well as in Ref. 22, is incompatible with the observed PL spectra, and a valid interpretation of the latter remains a theoretical challenge.

VI. CONCLUDING REMARKS

We have investigated the hole states in GaAs and InAs QDs doped with a single Mn impurity. A central-cell correction to the Coulomb potential of the acceptor, as well as the *sp-d* exchange interaction, has been taken into account. The principal results are the following. In spherical NCs the hole ground state retains its fourfold degeneracy, while the binding energy and the *sp-d* contribution to it increase with confinement. On the other hand, in lens-shaped self-assembled QDs, the highly anisotropic confinement leads to a drastic modification of the hole spectrum. The bulk ground state is split into two doublets. Although the binding energy increases with confinement as expected, it turns out to be lower than in the bulk in the low-confinement limit, where the ground state is heavy-hole-like with a smaller in-plane effective mass. With increasing in-plane confinement, in lattice-matched GaAs/(Ga,Al)As QDs, there is a crossover from a heavy-hole-like ground state to a light-hole-like one. In contrast, in strained InAs/GaAs QDs with a large strain-induced separation between the light- and heavy-hole bands, all the low-energy hole states are essentially derived from the latter and the first excitation energy is rather large. The hole density in SAQDs is a lot more spread out from the impurity center than in the bulk, and therefore the effective *sp-d* coupling strength is an order of magnitude smaller. Also, the level scheme of the exchange-induced fine structure is drastically different from that in the bulk. Our results clearly rule out any perturbative treatment of the confinement effects on the impurity states.

A preliminary study of the two-hole states suggests a singlet ground state in InAs/GaAs QDs of typical sizes. However, the excitonic spectrum resulting from such a configuration seems incompatible with the reported PL spectra.[8] Work is in progress for a more complete study of the relevant system consisting of two holes and one electron in interaction with the Mn impurity and will be reported elsewhere.

ACKNOWLEDGMENTS

We wish to thank O. Krebs and A. Lemaître for stimulating discussions. This work was partly supported by the Indo-French Centre for the Promotion of Advanced Research (IFCPAR) (Project No. 3604-1).

[1] K. Yanata, K. Suzuki, and Y. Oka, J. Appl. Phys. **73**, 4595 (1993); K. Yanata and Y. Oka, Jpn. J. Appl. Phys., Part 1 **34**, 164 (1995).
[2] A. A. Maksimov, G. Bacher, A. McDonald, V. D. Kulakovskii, A. Forchel, C. R. Becker, G. Landwehr, and L. Molenkamp, Phys. Rev. B **62**, R7767 (2000).
[3] S. Mackowski, T. Gurung, T. A. Nguyen, H. E. Jackson, L. M. Smith, G. Karczewski, and J. Kossut, Appl. Phys. Lett. **84**, 3337 (2004).
[4] R. N. Bhargava, D. Gallagher, X. Hong, and A. Nurmikko, Phys. Rev. Lett. **72**, 416 (1994).
[5] D. M. Hoffman, B. K. Meyer, A. I. Ekimov, I. A. Merkulov, Al. L. Efros, M. Rosen, G. Couino, T. Gacoin, and J. P. Boilot, Solid State Commun. **114**, 547 (2000).
[6] D. J. Norris, N. Yao, F. T. Charnok, and T. A. Kennedy, Nano Lett. **1**, 3 (2001).
[7] L. Besombes, Y. Léger, L. Maingault, D. Ferrand, H. Mariette, and J. Cibert, Phys. Rev. Lett. **93**, 207403 (2004).
[8] A. Kudelski, A. Lemaître, A. Miard, P. Voisin, T. C. M. Graham, R. J. Warburton, and O. Krebs, Phys. Rev. Lett. **99**, 247209 (2007).
[9] M. Linnarsson, E. Janzén, B. Monemar, M. Kleverman, and A. Thilderkvist, Phys. Rev. B **55**, 6938 (1997).
[10] D. G. Andrianov, V. V. Karataev, G. V. Lazareva, Yu. B. Muravlev, and A. S. Savel'ev, Fiz. Tekh. Poluprovodn. (S.-Peterburg) **11**, 1252 (1977) [Sov. Phys. Semicond. **11**, 738 (1977)].
[11] T. Dietl, H. Ohno, and F. Matsukura, Phys. Rev. B **63**, 195205 (2001).
[12] A. K. Bhattacharjee, Phys. Rev. B **51**, 9912 (1995).
[13] A. K. Bhattacharjee and C. Benoit à la Guillaume, Phys. Rev. B **55**, 10613 (1997).
[14] A. K. Bhattacharjee and J. Pérez-Conde, Phys. Rev. B **68**, 045303 (2003).
[15] F. V. Kyrychenko and J. Kossut, Phys. Rev. B **70**, 205317 (2004).
[16] A. O. Govorov and A. V. Kalameitsev, Phys. Rev. B **71**, 035338 (2005).
[17] J. Fernández-Rossier, Phys. Rev. B **73**, 045301 (2006).
[18] A. K. Bhattacharjee, Phys. Rev. B **76**, 075305 (2007).
[19] A. K. Bhattacharjee and C. Benoit à la Guillaume, Solid State Commun. **113**, 17 (2000).
[20] A. Baldereschi and N. O. Lipari, Phys. Rev. B **8**, 2697 (1973).
[21] A. O. Govorov, Phys. Rev. B **70**, 035321 (2004).
[22] J. I. Climente, M. Korkusinski, P. Hawrylak, and J. Planelles, Phys. Rev. B **71**, 125321 (2005).
[23] *Semiconductors: Data Handbook*, edited by O. Madelung (Springer-Verlag, Berlin, 2003).
[24] F. B. Pedersen and Y.-C. Chang, Phys. Rev. B **53**, 1507 (1996).
[25] P. Boucaud and S. Sauvage, C. R. Phys. **4**, 1133 (2003).

[26] L. He, G. Bester, and A. Zunger, Phys. Rev. B **70**, 235316 (2004).
[27] P. C. Sercel and K. J. Vahala, Phys. Rev. B **42**, 3690 (1990).
[28] C. Echeverría-Arrondo, J. Pérez-Conde, and A. K. Bhattacharjee, J. Appl. Phys. **104**, 044308 (2008).
[29] D. V. Bulaev and D. Loss, Phys. Rev. Lett. **95**, 076805 (2005).
[30] M. Ediger, G. Bester, A. Badolato, P. M. Petroff, K. Karrai, A. Zunger, and R. J. Warburton, Nat. Phys. **3**, 774 (2007).